THE JOURNAL OF COMPARATIVE NEUROLOGY 427:604–616 (2000)

Choline Acetyltransferase-Immunoreactive Neurons in the Developing Rat Retina

IN-BEOM KIM, EUN-JIN LEE, MUN-KYU KIM, DAE-KYOON PARK, AND MYUNG-HOON CHUN*
Department of Anatomy, College of Medicine, The Catholic University of Korea, Seoul 137-701, Korea

ABSTRACT

The development of cholinergic cells in the rat retina has been examined with immunocytochemistry by using antisera against choline acetyltransferase (ChAT). ChAT-immunoreactive (IR) cells were first detected at embryonic day 17 (E17) in the transitional zone between the neuroblastic layer (NBL) and ganglion cell layer (GCL). At E20, ChAT-IR cells are located exclusively in the GCL. At postnatal day 0 (P0), ChAT immunoreactivity appeared for the first time in cells at the distal margin of the NBL. Two prominent bands of labeled processes were first visible at P3, and by P15, these two bands resembled those of the adult retina. In addition, ChAT immunoreactivity appeared transiently in horizontal cells from P5 to P10. The number of ChAT-IR cells increased steadily up to P15. This resulted in a 93.8-fold increase between E17 and P15 (680–63,800 cells). However, after P15, the number declined by 19% from 63,800 cells at P15 to 51,800 in the adult. At all ages, the spatial density of each ChAT-IR cell population in the central retina was higher than in the periphery. In both central and peripheral regions, the peak density of ChAT-IR cells in the GCL was attained at E20. However, in the INL, the peak densities occurred at P3 in the central region and at P5 in the peripheral region. Up to P15, the soma diameter of ChAT-IR cells in the INL and GCL in each region increased continuously, reaching peak values at P15. Our results demonstrate that ChAT immunoreactivity is expressed in early developmental stages in the rat retina, as in other mammals, and that acetylcholine released from ChAT-IR cells may have neurotrophic functions in retinal maturation. J. Comp. Neurol. 427:604–616, 2000.

Indexing terms: cholinergic cells; development; immunocytochemistry

Acetylcholine (ACh) is present in all mammalian retinae studied to date and is now widely accepted as an excitatory neurotransmitter (for reviews, see Masland and Tauchi, 1986; Vaney, 1990; Wässle and Boycott, 1991). As revealed by immunocytochemistry with antisera against choline acetyltransferase (ChAT), which is the rate-limiting enzyme for the synthesis of ACh, the distribution and morphology of mammalian cholinergic amacrine cells is consistent across species. There are two subpopulations of cholinergic amacrine cells: one is found in the inner nuclear layer (INL) and the other forms a displaced population in the ganglion cell layer (GCL). Each population ramifies in the inner plexiform layer (IPL), where the dendritic plexus of amacrine cells from the INL is confined to sublamina a, and that of the displaced amacrine cells is confined to sublamina b (cat: Schmidt et al., 1985; Pourcho and Osman, 1986; rabbit: Famiglietti, 1983; Brandon, 1987; Famiglietti and Tumosa, 1987; rat: Voigt, 1986; Mitrofanis and Stone, 1988; Kim et al., 1998b; primate: Mariani and Hersh, 1988; Rodieck and Marshak, 1992; tree shrew: Conley et al., 1986, Sandmann et al., 1997). Furthermore, the distribution pattern of cholinergic amacrine cells in the mammalian retina mirrors the major features of the distribution of ganglion cells, with a maximal density at the area centralis and a decline toward the

Grant sponsor: Braintech 2000; Grant number: 98-J04-02-05-A-10; Grant sponsor: the Brain Korea 21 project.

*Correspondence to: Myung-Hoon Chun, Department of Anatomy, Catholic University Medical College, 505 Banpo-Dong, Socho-Ku, Seoul 137-701, Korea. E-mail: mhchun@cmc.cuk.ac.kr

Received 13 March 2000; Revised 14 August 2000; Accepted 14 August 2000

periphery (cat: Schmidt et al., 1985; Pourcho and Osman, 1986; rabbit: Vaney et al., 1981; Famiglietti and Tumosa, 1987; rat: Voigt, 1986; Mitrofanis and Stone, 1988; primate: Rodieck and Marshak, 1992; tree shrew: Sandmann et al., 1997).

To improve our understanding of cholinergic amacrine cells, several developmental studies have been undertaken in different mammalian species (cat: Dann, 1989; Mitrofanis et al., 1989; rabbit: Wong and Collin, 1989; rat: Puro et al., 1982; Mitrofanis et al., 1988). In a biochemical study of the rat retina, Puro et al. (1982) reported that ACh was first synthesized at embryonic day 16 (E16) and that ChAT activity was detected consistently by E16. This finding suggested that cholinergic amacrine cells appear in early developmental stages. In the cat retina, ChAT-immunoreactive (ChAT-IR) cells first appear at E56 (Mitrofanis et al., 1989) and in the rabbit retina, cholinergic amacrine cells are morphologically distinguishable at birth when they constitute two subpopulations, one in the INL and the other in the GCL (Wong and Collin, 1989). However, in the rat retina, Mitrofanis et al. (1988) reported that cholinergic amacrine cells were not detected until postnatal day 15 (P15), whereas Kim et al. (1998a) claimed that cholinergic amacrine cells of the rat retina were already labeled by antisera against ChAT during early postnatal development. This discrepancy could be due to a difference in type of rat used, the methods, or the sensitivity of the antisera.

The rat has recently been used more extensively as an experimental animal in retinal research, since many of the transmitter receptors have been cloned for the rat and rat retinae are more readily available for in vitro physiology (Boycott and Wässle, 1999). Therefore, the present study was undertaken to reexamine in detail the development of cholinergic amacrine cells in the rat retina. For this purpose, antiserum against ChAT was applied to radial vibratome sections of the retina and to retinal wholemount preparations. This permits a quantitative analysis of cholinergic amacrine cells with respect to their retinal topography, spatial density distribution, and relative distribution within the INL and GCL.

MATERIALS AND METHODS

Animals

Sprague-Dawley rats were used for this study. The animals were treated according to the regulation of the Catholic Ethics Committee of the Catholic University of Korea, Seoul, in conformity with all NIH guidelines. Female rats were mated and pregnancy was determined by examination of the vaginal plug; the next day was deemed embryonic day 0 (E0). The animals were maintained on a daily cycle of 12-hour dim light and 12-hour darkness. The day of birth was counted as postnatal day 0 (P0).

Tissue preparation

Pups at E15, E16, E17, E18, E20, P0, P1, P3, P5, P7, P10, P15, and P21, as well as adult rats, were anesthetized by intraperitoneal injection of 4% chloral hydrate (1 ml/100 g body weight) and killed by an overdose (4 ml/100 g body weight) of the same anesthetic. The eyes were enucleated and opened by an encircling cut, and the posterior eyecups were immersion fixed for 30 minutes in 4% paraformaldehyde in 0.1 M phosphate buffer (PB; pH 7.4) containing 0.2% picric acid. The left eyes were used for wholemount preparations and the right for vertical sections. The superior surface of each eyeball was marked with a felt pen and later by an incision for orientation. Subsequently, the retinae were dissected carefully from the choroid and further fixed by immersion in the same fixative for 2 hours at 4°C. Following fixation, the retinae were transferred to 30% sucrose in PB for 8 hours at 4°C. Retinae were then frozen in liquid nitrogen, thawed, and rinsed in 0.01 M phosphate-buffered saline (PBS; pH 7.4). For vertical sections, retinal pieces taken from the superior region were embedded in 4% agar (Merck, Darmstadt, Germany) and then sectioned vertically with a vibratome at a thickness of 40 μm. After several washes in PBS, the retinae were stored at 4°C for further use.

Immunocytochemistry

Immunostaining was performed by using the indirect antibody method. Wholemount preparations and 40-μm-thick vibratome sections were incubated in 10% normal donkey serum (NDS) in PBS containing 1% Triton X-100 for 1 hour at room temperature. Wholemount preparations were incubated in goat polyclonal antisera against ChAT (dilution 1:300; Chemicon, Temecula, CA) in PBS containing 0.5% Triton X-100 for 48 hours at 4°C, and vibratome sections were incubated for 8 hours at 4°C. After washing in PBS for 45 minutes (3 × 15 minutes), wholemount preparations were incubated for 12 hours at 4°C in peroxidase-labeled anti-goat IgG (dilution 1:100; Jackson ImmunoResearch, West Grove, PA) in PBS containing 0.5% Triton X-100, and vibratome sections were incubated for 2 hours at room temperature. The retinae were rinsed in two changes of PBS and three changes of 0.05 M Tris-HCl buffer (TB; pH 7.4) for 5 minutes at room temperature, before incubation in 0.05% 3,3′-diaminobenzidine tetrahydrochloride (DAB) in TB for 10 minutes. Hydrogen peroxide was added to the incubation medium to make a final concentration of 0.01% H_2O_2, and the container was shaken gently as the reaction proceeded. After 1–2 minutes, as determined by the degree of staining, the reaction was stopped with several washes of TB and PB. The retinae were collected on 0.5% gelatin-coated slides with the ganglion cell layer facing up, mounted in glycerol, and coverslipped.

Cell count, density mapping, and soma size analysis

The total cell number of both the conventional amacrine population in the INL and the displaced population in the GCL was counted in two to four retinal wholemount preparations from each group. Wholemount preparations were mapped systematically in 1-mm steps by using a calibrated eyepiece graticule. The data were recorded as density maps in order to identify the distribution patterns of labeled amacrine cells and displaced amacrine cells during developmental stages. The mean density of the labeled amacrine and displaced amacrine cells was calculated by dividing the total number of cells by the retinal area in both central and peripheral regions of the retina. A region within half of the diameter from the optic disc of the retina was considered as a central region, whereas the rest of the retina was considered as a peripheral region.

Using an image analyzer (BMI-PLUS; Bummi Universe, Ansan, Korea), soma size was measured in 50 cells from the following populations of ChAT-IR cells: amacrine

and displaced amacrine cells located in both central (including putative area centralis) and peripheral regions (temporal and nasal margins) of the retina. The soma sizes were averaged to give a representative mean value. The results are not corrected for the negligible shrinkage of the tissue during the mounting process.

RESULTS

Morphology of ChAT-IR cells

Salient features in the development in morphology of ChAT-immunoreactive (ChAT-IR) cells, determined from vertical vibratome sections and wholemount preparations, are illustrated in Figures 1–4. ChAT immunoreactivity was first detected at E17, in a population of putative displaced cholinergic neurons in the central retina near the optic disc (Figs. 1A, 3A). Their somata were located in the transitional zone between the neuroblastic layer (NBL) and the GCL, with one to two short stem dendrites emerging from the somata and ramifying in the IPL (Fig. 1A). At E18, ChAT-IR displaced amacrine cells with increased density were seen only in the central region of the retina (data not shown). At E20, ChAT immunoreactivity became considerably stronger in the central region, and ChAT-IR somata were localized clearly to the GCL (Fig. 1B). In wholemount preparations, these cells began to assume stellate morphology (Fig. 3B). In the peripheral region, ChAT-IR cells of the GCL were first visible at this time (Fig. 3C), and their features were similar to those of ChAT-IR cells located in the central region at E17 and E18.

At P0, ChAT immunoreactivity was first detected in the distal part of the NBL in a population of conventional cholinergic amacrine cells (Fig. 1C). The immunoreactivity was observed mainly in a restricted region of the soma where the primary dendrite originates. Therefore, the complete shape of the soma was hardly observed, and the processes could not be followed into the IPL. At P1, the somata of ChAT-IR cells in the NBL became more apparent (Figs. 1D, 4B). However, a few labeled somata were difficult to trace because of their weak immunoreactivity (Fig. 4B). Prior to P3, ChAT-IR processes were observed only in the vicinity of ChAT-IR somata and were readily traced to an individual soma. At P3, two continuous, distinct bands of ChAT-IR processes were visible in the outermost and innermost strata of the IPL (Fig. 1E). At P5, somata of two populations of ChAT-IR cells with strong immunoreactivity were observed in the INL and GCL (Fig. 1F). These cells had a primary dendrite with a short, stout stalk, and their processes formed two distinct bands, each generally lying in the middle region of sublamina a and b of the IPL (Fig. 1F). From postnatal day 5 onward, the somata of the two populations of ChAT-IR cells in the INL and GCL were easily distinguished in wholemount preparations (Figs. 4C-H). In addition, weak ChAT immunoreactivity was expressed from P5 to P10 in the outer plexiform layer (OPL) by cells with somata located in the outermost part of the INL (Figs. 1F, 2A). These cells were identified as horizontal cells by Kim et al. (1998a). At P10, two distinct bands of ChAT-IR processes were observed in the outer third and in the inner third of the IPL, respectively (Fig. 2A).

Figure 2B shows a vertical vibratome section of a 15-day-old rat retina processed for ChAT immunoreactivity. At this time, primary dendrites of ChAT-IR cells in the INL and GCL became thinner and their processes stratified in stratum 2, and in strata 3 and 4 of the IPL, respectively, as shown in both the 21-day-old and adult rat (Fig. 2C).

Number of ChAT-IR cells

The total number of ChAT-IR cells in the INL and GCL were counted in two to four wholemount preparations at each developmental stage (Fig. 5A; Table 1). The number of ChAT-IR cells increased steadily up to P15. This resulted in a 93.8-fold increase between E17 and P15 (680 cells to 63,800 cells, respectively), with a 38.8-fold increase between E17 and P1 (680 cells to 26,400 cells, respectively). However, after P15, the number declined by approximately 19%, from 63,800 cells at P15 to 51,800 cells in the adult.

When the GCL and INL were examined separately, there was a 44.3-fold increase in the GCL population between E17 and P15 (680 cells to 30,100 cells, respectively), with a 22.4-fold increase between E17 and P1 (680 cells to 15,200 cells, respectively). Since ChAT-IR cells in the INL were first visible at P0 and, at this stage, ChAT-IR cells in the INL were hardly distinguished from those in the GCL, the total number of ChAT-IR cells could be determined from P1 onwards. At P1, the number of ChAT-IR cells in the INL was already 11,300, suggesting that there was an enormous increase between E20 and P1. In the INL, there was a 3.0-fold increase between P1 and P15 (11,300 cells to 33,700 cells, respectively), indicating that increase of cell numbers is higher in the INL than in the GCL, with about a 2.0-fold increase between P1 and P15.

In conclusion, the number of ChAT-IR cells increased in both populations with the most marked increase occurring during the perinatal period up to P15. Thereafter, the number of ChAT-IR cells declined gradually in both populations.

Density and distribution of ChAT-IR cells

The spatial densities of developing ChAT-IR cells in the INL and GCL were determined from E17 to the adult (Fig. 5B; Table 1). The mean density was calculated by dividing the total number of cells by the retinal area. At E17, the cell density in central region of the retina was approximately 1,260 cells/mm^2, increasing to 1,950 cells/mm^2 at E20, and reaching a peak value of 2,550 cells/mm^2 at P1. After P1, the density decreased continuously until adulthood, when it was approximately 1,200 cells/mm^2, with the greatest decrease occurring between P15 and adult (2,100 to 1,200 cells/mm^2, respectively).

In the retinal periphery, the cell density increased from 1,250 cells/mm^2 at E20 to 2,100 cells/mm^2 at P3, and after P3 the cell density decreased gradually to a value of 920 cells/mm^2 in the adult, with the steepest decline occurring between P15 and adult (2,000 to 920 cells/mm^2, respectively), thereby showing a similar pattern to the central region.

The spatial distribution patterns of postnatally developing ChAT-IR cells in the INL and GCL from P1 to the adult are presented as density maps (Figs. 6, 7). ChAT-IR cells were distributed throughout the whole retina except at E17, when they were not observed at the peripheral margins of the retina. From E17, the density of ChAT-IR cells was highest in the region immediately temporal and

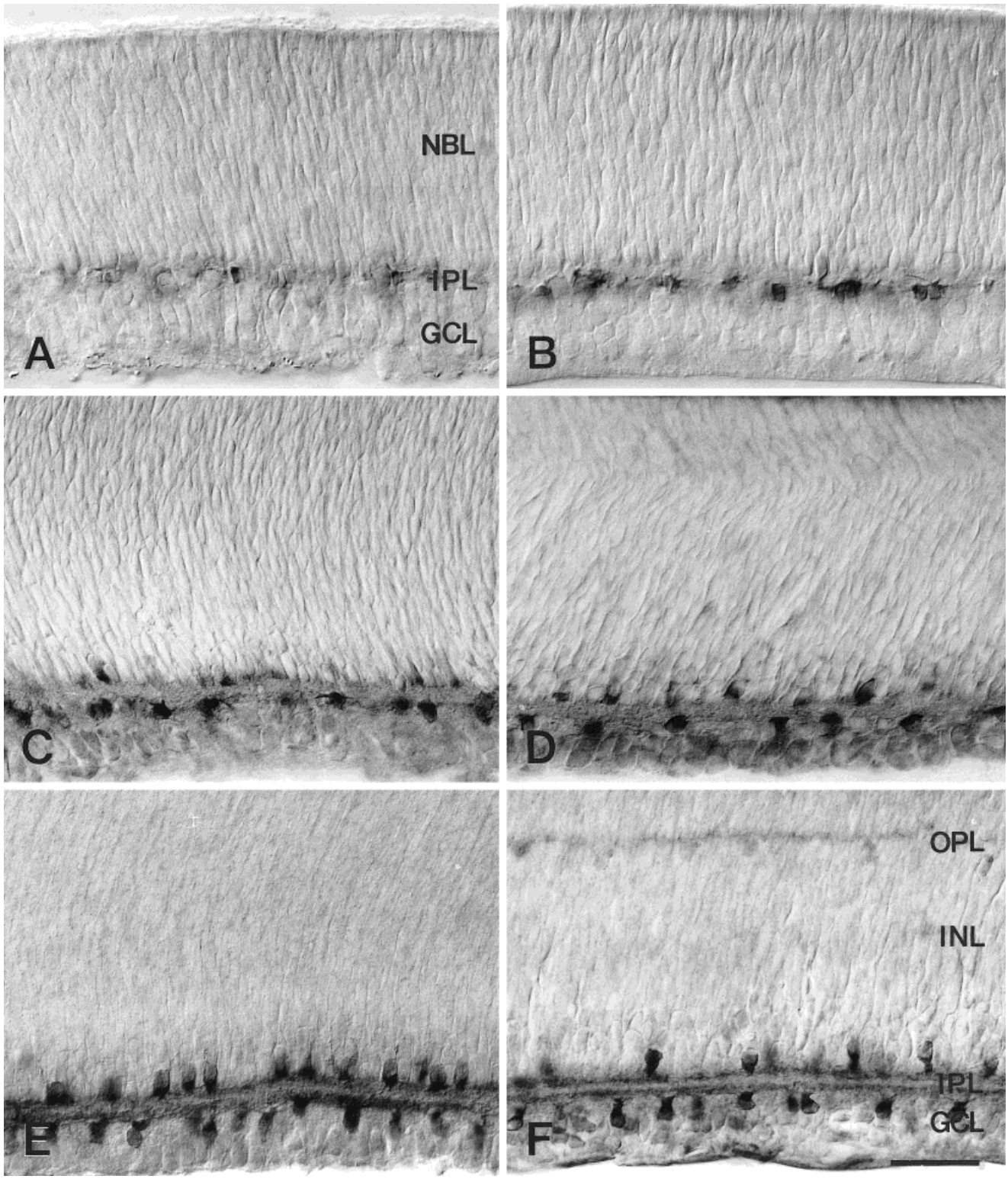

Fig. 1. Photomicrographs showing retinal vibratome sections processed for ChAT immunocytochemistry in developing retinae at E17 (A), E20 (B), P0 (C), P1 (D), P3 (E), and P5 (F). **A:** ChAT immunoreactivity is seen in cells located in the transitional zone between the neuroblastic layer (NBL) and the ganglion cell layer (GCL). **B:** ChAT-immunoreactive cells are seen in the outermost region of the GCL. **C:** In addition to labeled displaced amacrine cells, ChAT immunoreactivity is visible in the restricted parts of the cells located in the inner margin of the NBL. **D:** Stronger immunoreactivity is seen in the cells located in the NBL. **E,F:** Processes originating from somata located in both layers form two prominent bands in the inner plexiform layer (IPL). OPL, outer plexiform layer. Scale bar = 50 μm.

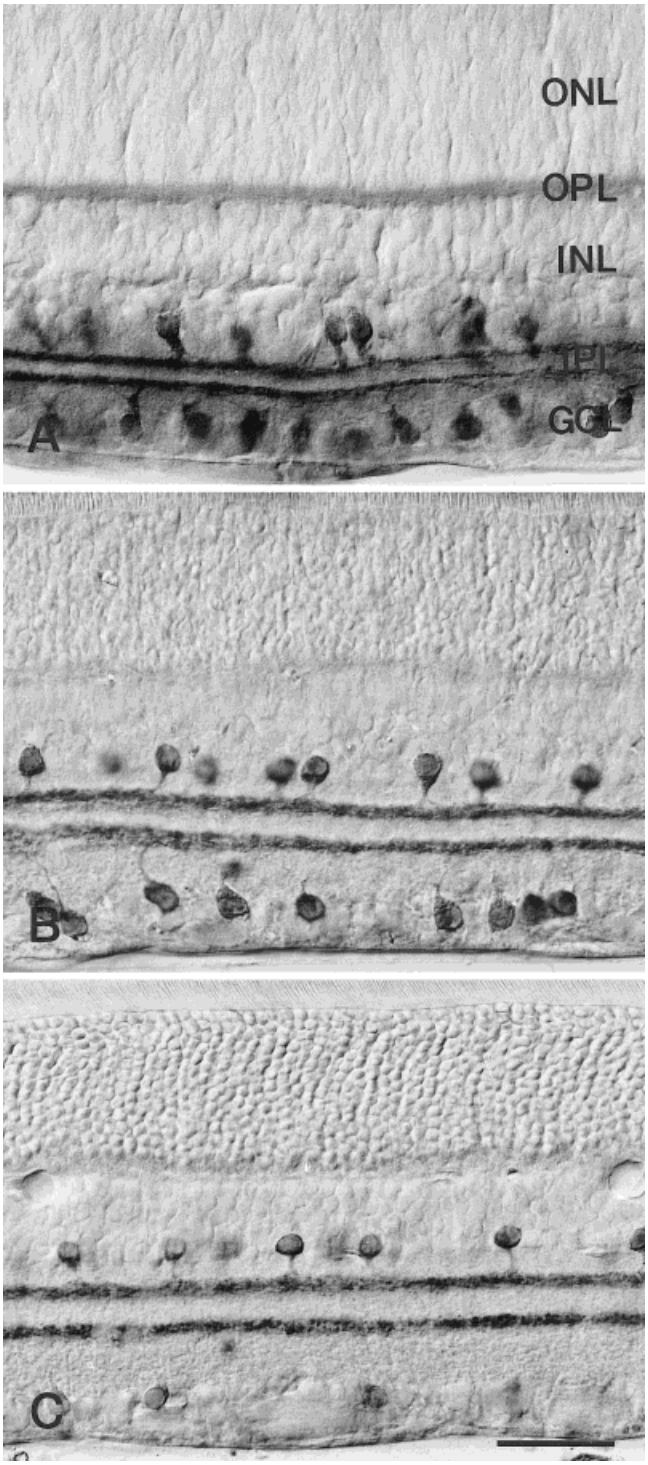

Fig. 2. Photomicrographs showing retinal vibratome sections processed for ChAT immunocytochemistry in developing retinae at P10 (A) and P15 (B) and in the adult retina (C). **A:** Stout primary dendrites originate from somata located in the inner nuclear layer (INL) and ganglion cell layer (GCL) and stratify in sublaminae a and b of the inner plexiform layer (IPL), forming a prominent band. Morphological features of the ChAT-labeled cells shown in **B** are quite similar to those shown in **C**. ONL, outer nuclear layer; OPL, outer plexiform layer. Scale bar = 50 μm.

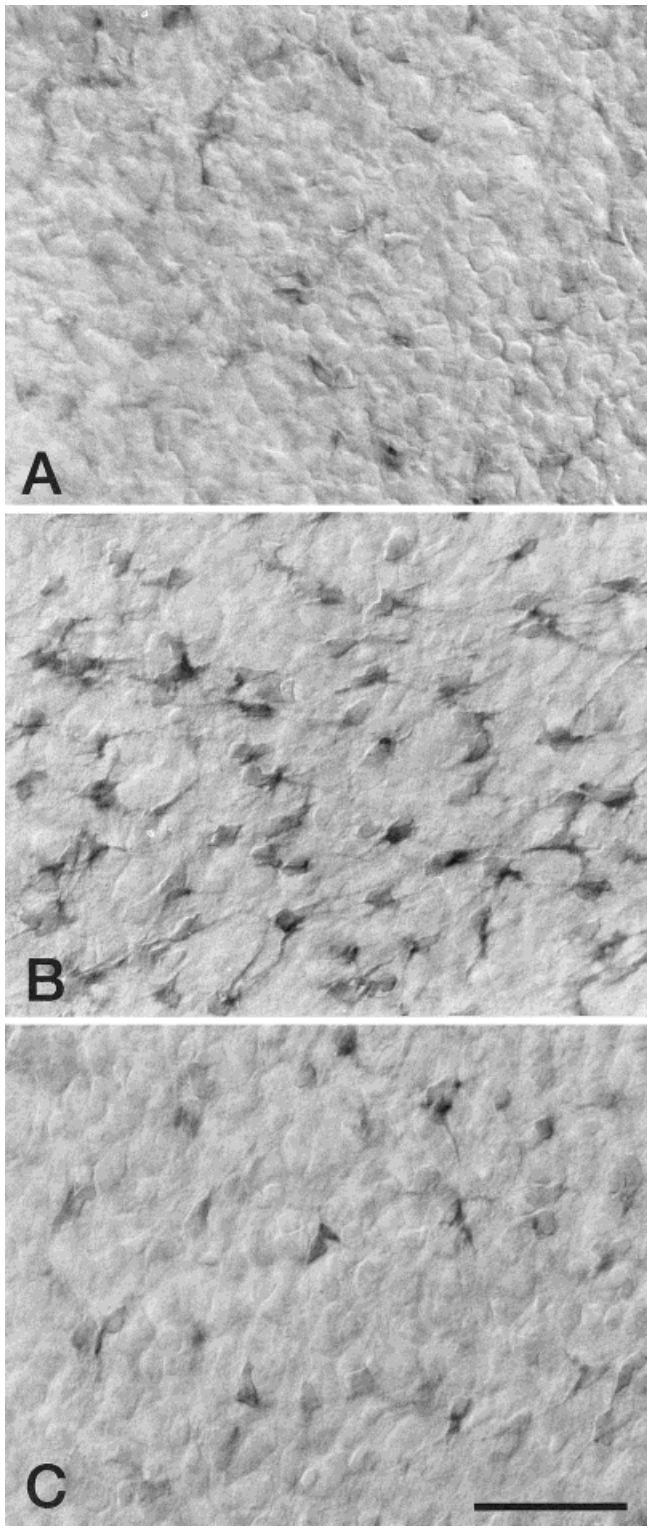

Fig. 3. Photomicrographs showing the GCL of wholemount preparations processed for ChAT immunocytochemistry in developing retinae at E17 (A) and E20 (B, C). **A:** Photomicrograph taken from the central retina showing ChAT-immunoreactive cells. **B,C:** Photomicrographs taken from central and peripheral regions, respectively. In B, two or three short processes are seen to originate from the somata of stellate ChAT-immunoreactive cells. These cells are In C, the shape of ChAT-immunoreactive cells is similar to that shown in A. Scale bar = 50 μm.

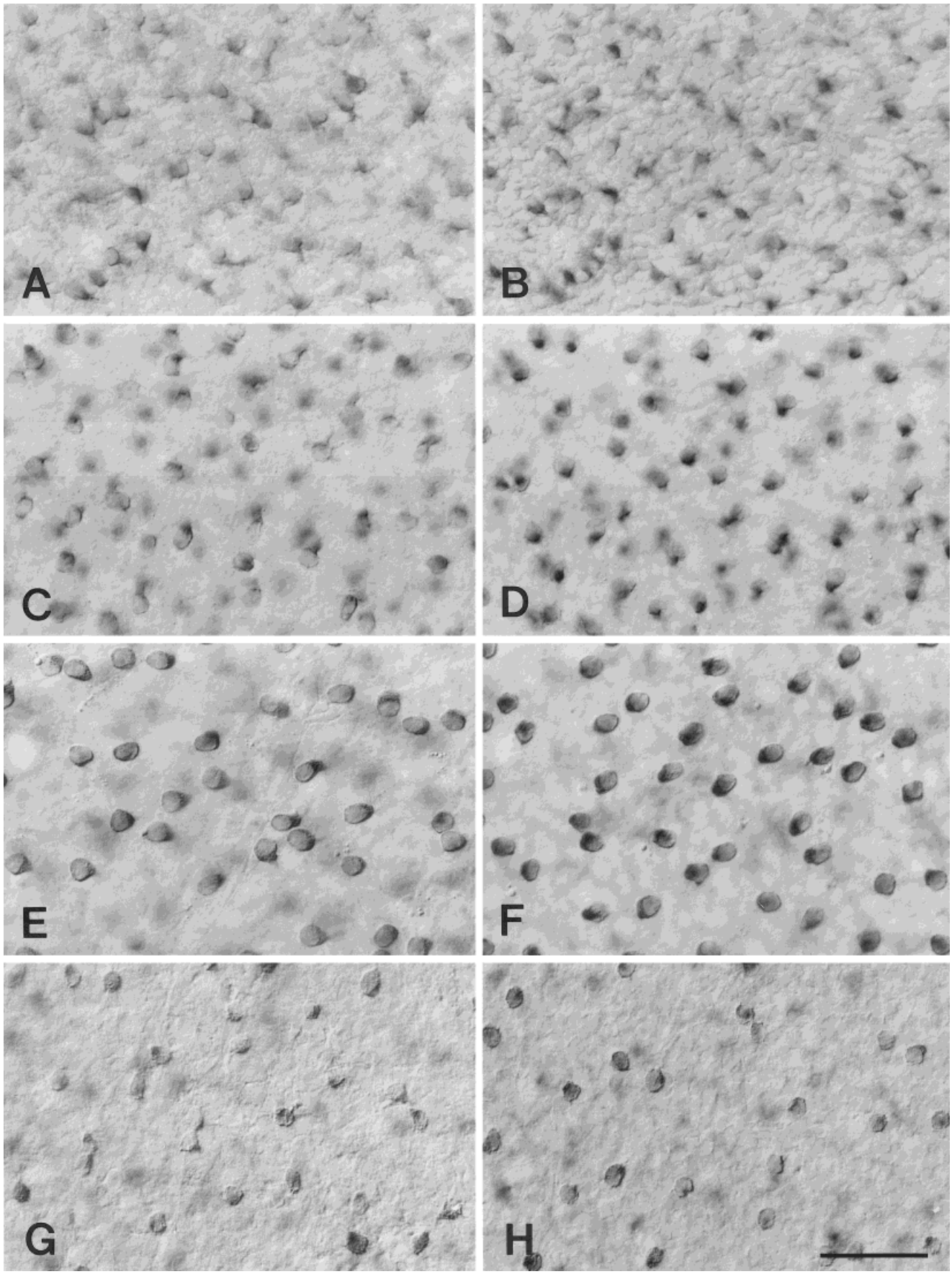

Fig. 4. Photomicrographs taken from regions showing peak cell density of wholemount preparations processed for ChAT immunocytochemistry in developing retinae at P1 (A, B), P5 (C, D), and P15 (E, F) and adult retina (G, H). A, C, E, and G are taken from the GCL, and B, D, F, and H are taken from the INL. **A,B:** Compared with ChAT-IR cells in the GCL, some labeled cells in the INL are not well defined. **C,D:** Somata of ChAT-labeled cells are well defined in the INL and GCL. **E,F:** Strongly labeled cells are seen clearly. **G,H:** The density of ChAT-labeled cells seems to be low compared with that shown in E and F. Scale bar = 50 μm.

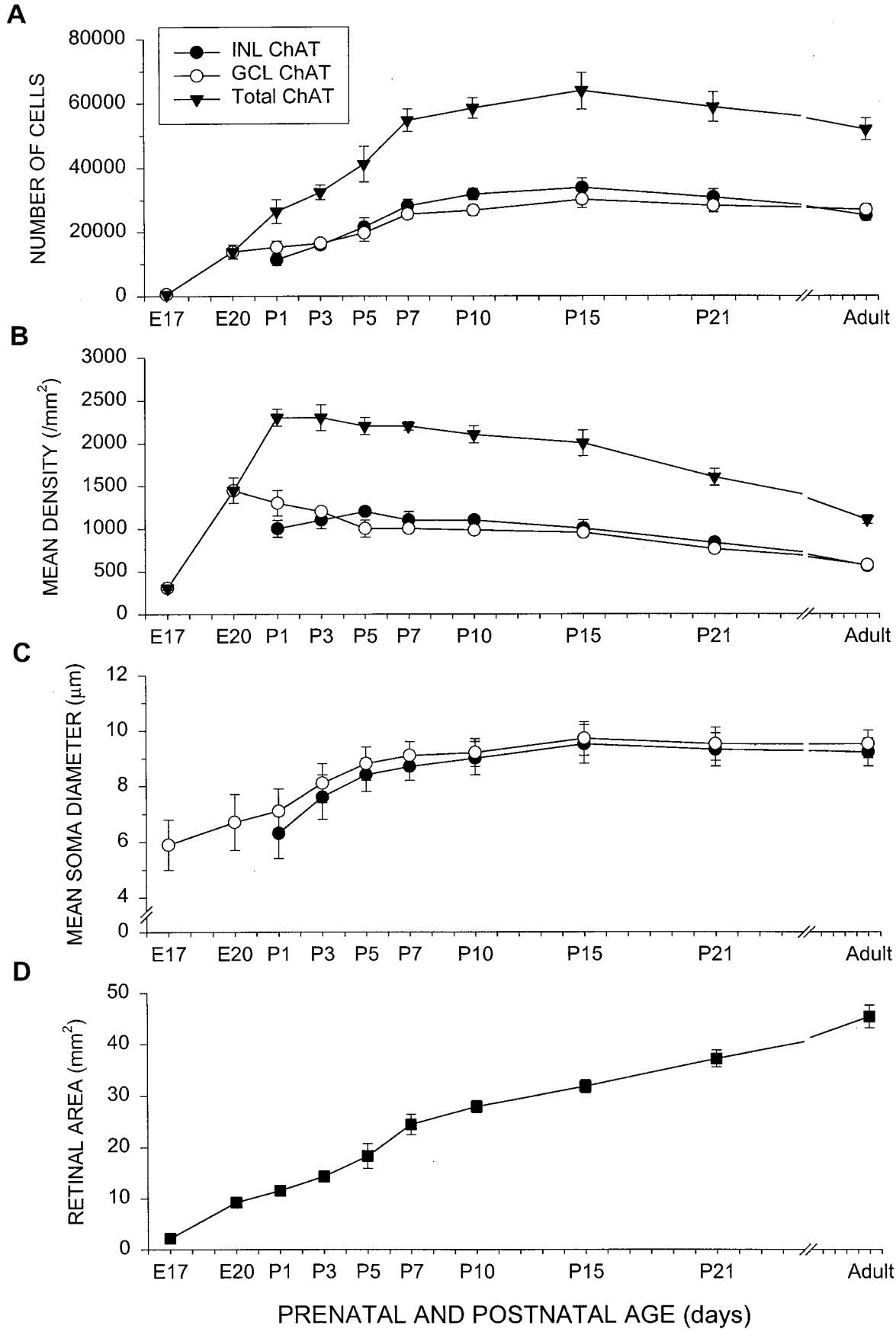

Fig. 5. Developmental features according to number (**A**), spatial density (**B**), and soma sizes (**C**) of ChAT-immunoreactive cells, as well as the changing retinal area (**D**), are plotted at various developmental stages.

TABLE 1. Retinal Area, Number, Mean Density, and Soma Diameter of ChAT-IR Amacrine Cells in the Developing and Adult Rat Retinae

	E17	E20	P1	P3	P5	P7	P10	P15	P21	Adult
Retinal area (mm^2)	2.0–2.5	8.0–10.0	10.0–13.0	13.5–15.0	15.5–21.0	22.0–27.0	26.0–29.5	29.5–33.5	35.0–39.0	42.0–48.0
Number of cells in thousands										
INL ChAT	—	—	9.4–13.1	14.0–17.3	18.2–25.0	25.6–30.6	28.0–34.0	31.1–37.1	28.2–33.2	22.2–27.1
GCL ChAT	0.63–0.72	10.9–16.3	13.2–17.2	15.2–17.5	16.4–23.1	23.4–27.6	24.6–29.6	27.6–33.1	26.0–30.3	23.6–29.5
Total ChAT	0.63–0.72	10.9–16.3	22.6–30.3	29.2–34.8	34.7–48.0	49.0–58.6	52.6–63.6	57.4–70.2	54.2–63.5	45.8–55.6
Mean density in thousands ($/mm^2$)										
INL ChAT										
Central	—	—	1.1–1.3	1.2–1.5	1.2–1.4	1.1–1.3	1.0–1.2	0.98–1.2	0.81–0.92	0.54–0.63
Peripheral	—	—	0.64–0.95	0.95–1.1	0.94–1.1	0.90–1.0	0.88–1.0	0.85–1.0	0.73–0.84	0.42–0.52
Mean	—	—	0.92–1.1	1.0–1.2	1.1–1.2	1.1–1.2	1.1–1.2	1.0–1.1	0.80–0.86	0.53–0.59
GCL ChAT										
Central	1.2–1.3	1.8–2.1	1.2–1.6	1.0–1.4	1.0–1.2	1.0–1.2	0.96–1.1	0.95–1.1	0.78–0.85	0.55–0.64
Peripheral	—	1.1–1.4	0.96–1.4	0.96–1.2	0.90–1.1	0.86–1.0	0.82–1.0	0.80–0.97	0.65–0.74	0.43–0.52
Mean	0.29–0.33	1.3–1.7	1.1–1.4	1.1–1.2	1.0–1.1	1.0–1.1	0.94–1.0	0.93–0.98	0.73–0.79	0.54–0.60
Total ChAT										
Central	1.2–1.3	1.8–2.1	2.3–2.8	2.3–2.8	2.2–2.6	2.2–2.5	2.0–2.4	1.9–2.3	1.6–1.8	1.1–1.3
Peripheral	—	1.1–1.4	1.6–2.1	1.9–2.3	1.8–2.2	1.8–2.0	1.7–2.0	1.7–2.0	1.4–1.6	0.84–1.0
Mean	0.29–0.33	1.3–1.7	2.2–2.4	2.2–2.4	2.2–2.3	2.2–2.3	2.0–2.2	1.9–2.1	1.5–1.6	1.1–1.2
Mean soma diameter (μm)										
INL ChAT										
Central	—	—	6.3	7.5	8.2	8.5	8.7	9.2	9.1	9.0
Peripheral	—	—	6.4	7.8	8.6	8.9	9.2	9.7	9.6	9.4
Mean	—	—	6.3	7.6	8.4	8.7	9.0	9.5	9.3	9.2
GCL ChAT										
Central	5.9	6.8	7.0	8.0	8.5	8.8	9.0	9.4	9.3	9.2
Peripheral	—	6.6	7.1	8.2	8.9	9.2	9.4	9.9	9.8	9.7
Mean	5.9	6.7	7.1	8.1	8.7	9.0	9.2	9.7	9.5	9.5

superior to the optic disc. Relatively high cell densities extended from this area to the optic disc, and there was a gradual decline in density toward the peripheral retina (Figs. 6, 7). The cell density was generally lowest in the inferonasal region, as shown in Figures 6 and 7.

At all ages, the density of the ChAT-IR cell population in the central region was higher than that in the peripheral region (Figs. 6, 7; Table 1). In both central and peripheral regions, the peak density of ChAT-IR cells in the GCL was attained at E20 (Table 1). However, in the INL, the peak densities were reached at P3 in central region and at P5 in peripheral region (Table 1).

Soma size of ChAT-IR cells

Soma sizes were determined for ChAT-IR cells of the INL and GCL in central and peripheral retina. Fifty well-labeled cells were measured in both layers at each retinal location, making a total sample size of 200 cells for each animal at each stage (Fig. 5C; Table 1). Before P1, due to indistinct boundaries, the difficulty of tracing the somata of ChAT-IR cells in the INL impeded soma size analysis by using wholemount preparations.

In the adult rat retina, confirming a previous study (Voigt, 1986), there were no significant differences ($P > 0.05$) between the diameters of ChAT-IR somata in the INL and those in the GCL in central and peripheral regions. The mean soma diameter differed only by 0.3 μm (Fig. 5C; Table 1). Furthermore, there were no significant differences ($P > 0.05$) between the central and peripheral regions in each layer. The mean soma diameter differed only by 0.4 and 0.5 μm, respectively (Table 1).

Up to P15, the soma diameter of ChAT-IR cells in the INL and GCL of each region increased continuously, reaching a peak value at P15. The mean soma diameter of ChAT-IR cells located in the INL was 6.3 μm at P1; 7.6 μm at P3; 8.4 μm at P5; 8.7 μm at P7; 9.0 μm at P10; 9.5 μm at P15, and 9.3 μm at P21 (Fig. 5C; Table 1). In the GCL, the mean soma diameters of ChAT-IR cells in both regions were slightly larger than in the INL in equivalent regions of retina. The mean diameter of ChAT-IR cells located in the GCL was 5.9 μm at E17; 6.7 μm at E20; 7.1 μm at P1; 8.1 μm at P3; 8.7 μm at P5; 9.0 μm at P7; 9.2 μm at P10; 9.7 μm at P15, and 9.5 μm at P21 (Fig. 5C; Table 1). At all developmental stages examined, the mean soma diameters of ChAT-IR cells in both layers in the central retina were slightly smaller than those in the peripheral retina, except at E20. For each developmental group, there were no significant differences ($P > 0.05$) between the soma diameters of ChAT-IR cells in the central and peripheral regions of each layer. Furthermore, either centrally or peripherally, there were no significant differences ($P > 0.05$) between the soma diameters of ChAT-IR cells in the INL and GCL. However, soma diameters of ChAT-IR cells in both layers of each region were significantly larger ($P < 0.05$) during developmental periods between E17 and E20, P1 and P3, P3 and P5, and P10 and P15 (Table 1).

DISCUSSION

We have studied the development of cholinergic cells in the rat retina by using antisera against ChAT. The detailed developmental changes in cholinergic neurons have been clarified by identifying their time of appearance, their morphological differentiation, and the changing numbers of cells and their distribution.

Timing of advent of ChAT-IR cells

The present study has shown that ChAT immunoreactivity is present in the central region of the rat retina at E17, in good agreement with a previous biochemical study by Puro et al. (1982), who reported that ACh is first synthesized at E16 and ChAT activity is detected reproducibly by E16. In addition, our results further confirm the immunocytochemical studies by Koulen (1997) and Kim et al. (1998a), which reported that a vesicular acetylcholine transporter—reflecting the ChAT-IR phenotype—first appears at birth. However, our results contrast with those of Mitrofanis et al. (1988), who reported that ChAT-IR amacrine cells do not appear in the rat retina

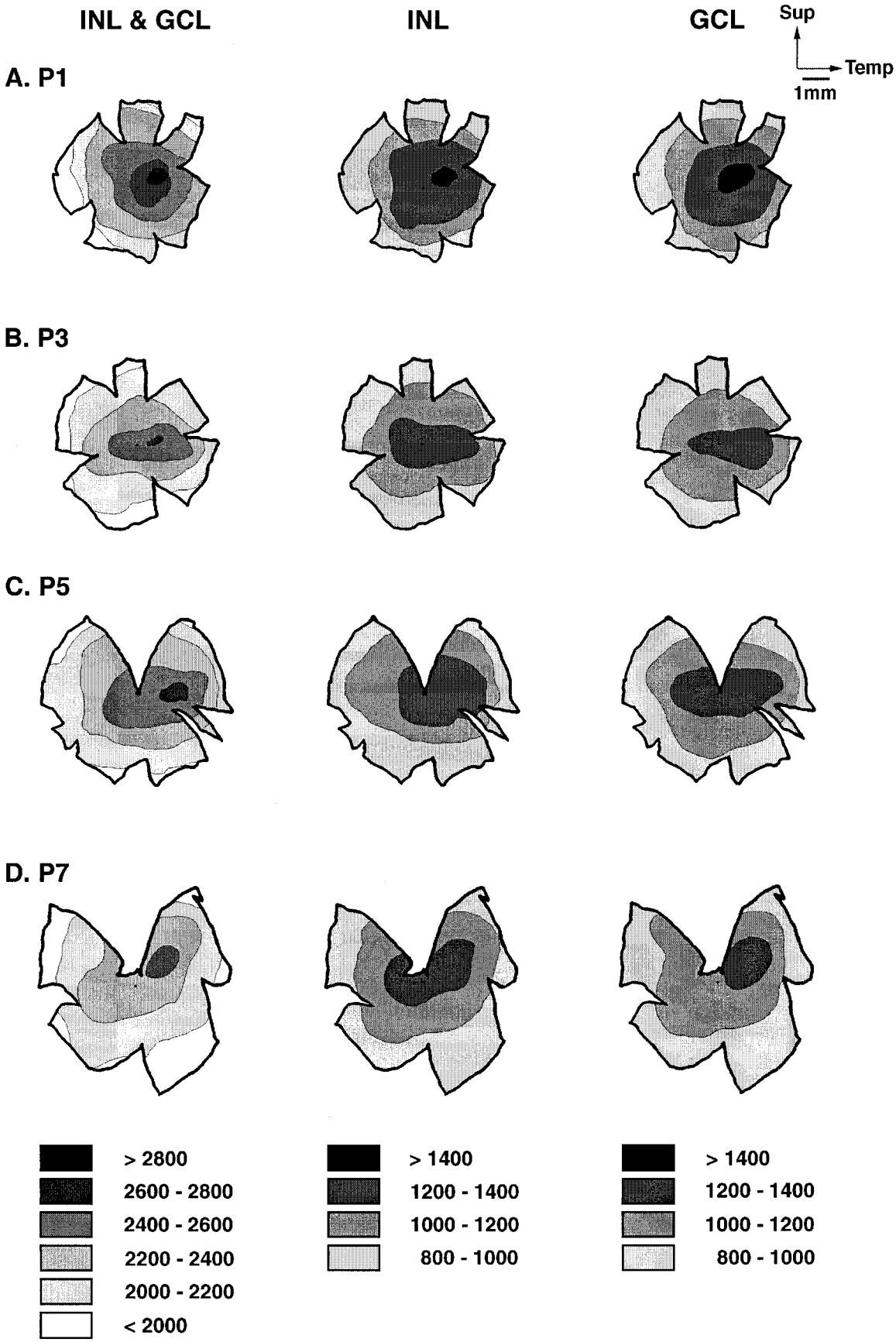

Fig. 6. **A–D:** Maps showing the distribution of ChAT-immunoreactive cells in a single retina for each developmental stage. The highest density is seen in the superior temporal region of the retina. A small black dot in the center indicates the optic disc of the retina.

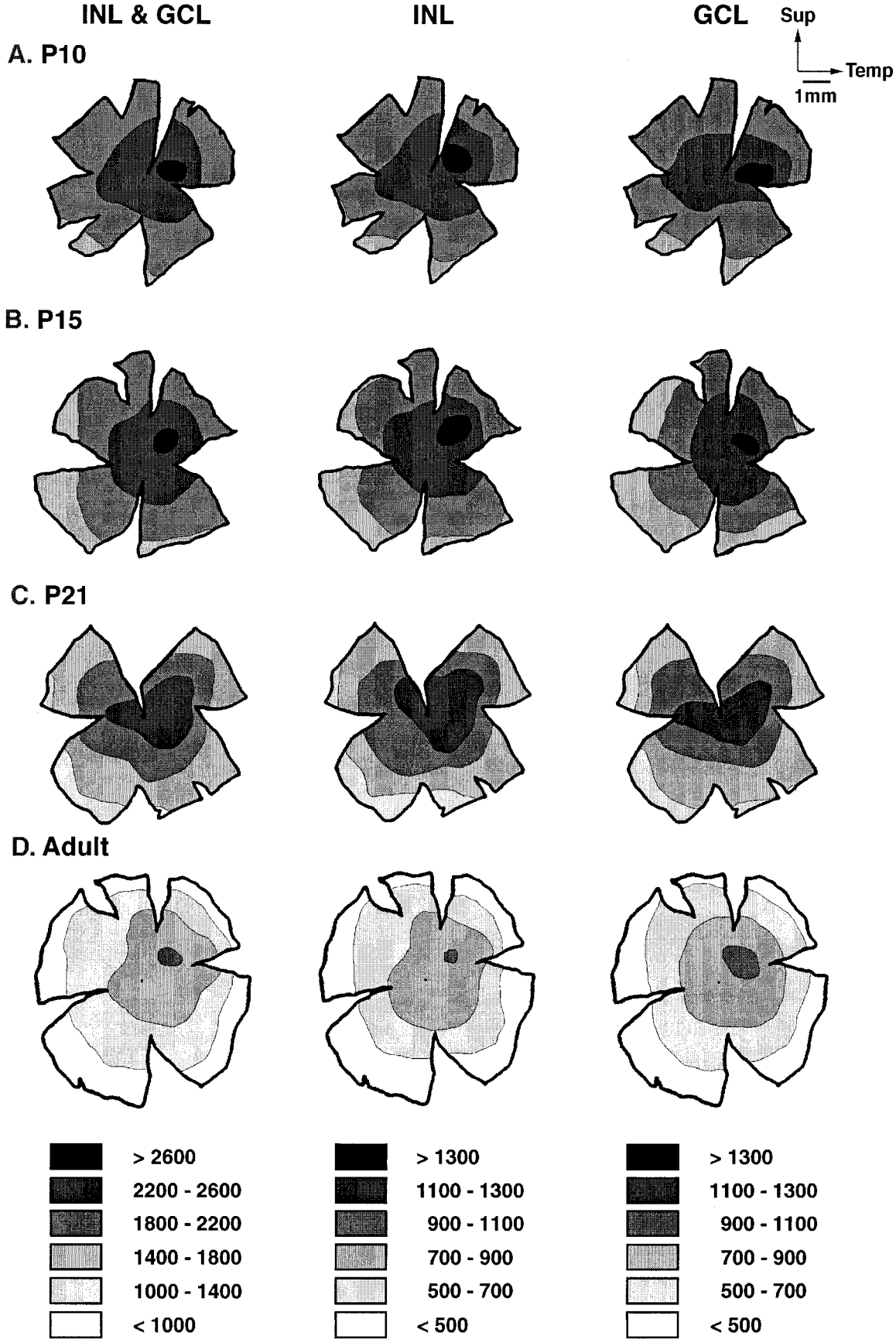

Fig. 7. **A–D:** Maps showing the distribution of ChAT-immunoreactive cells in a single retina for each age. The highest density is seen in the superior temporal region of the retina. A small black dot in the center indicates the optic disc of the retina.

until P15. This discrepancy is probably due to differences in species, methods, or the sensitivity of the antisera used.

This early appearance of ChAT-IR amacrine cells has also been reported in other mammalian retinae. In the cat retina, ChAT-IR cells first appear at E56 (Mitrofanis et al., 1989), and, in the rabbit retina, these cholinergic amacrine cells are morphologically distinguishable at birth when they constitute two distinct subpopulations, one in the INL and the other in the GCL (Wong and Collin, 1989). Thus, the early appearance of ChAT-IR cells during development is a common phenomenon in the mammalian retina.

Development of ChAT-IR amacrine cells

The population of displaced ChAT-IR amacrine cells was first observed in the central region of the rat retina near the optic disc at E17, at a time when the differentiation of ganglion cells as a distinct layer is beginning adjacent to the optic nerve (Braekevelt and Hollenberg, 1970). The population of conventional ChAT-IR cells was first observed at P0. These results may indicate that the expression of ChAT occurs earlier in neurons located in the GCL than in the INL. Recently, a similar differential expression was also reported in the opossum retina (Camargo et al., 1999), unlike the cat retina, in which both populations of ChAT-IR amacrine cells were observed simultaneously at E56 (Mitrofanis et al., 1989). This earlier expression of ChAT-IR in displaced amacrine cells suggests that ACh has an effect on retinal ganglion cells from the earliest time. Support for this view comes from the following facts: 1) ganglion cells are invariably the first retinal cells to be born (Cepko, 1993; Cepko et al., 1996); 2) rabbit retinal ganglion cells are responsive to ACh at birth or shortly thereafter (Masland, 1977); and 3) ACh is the major excitatory input onto ganglion cells in the developing retina, acting via nicotinic receptors and affecting the spontaneous bursting activity of these cells (Feller et al., 1996; Sernagor and Grzywacz, 1996).

In the present study, both conventional and displaced ChAT-IR cells can be identified at P0. These cholinergic cells attain a near-adult appearance by P15, i.e., around the time of eye opening, which varies individually between P13 and P15. This finding is in good agreement with the previous report by Koulen (1997), who has shown similar developmental processes in the rat retina. In the tree shrew retina, cholinergic cells were also shown to have an adult-like appearance by P19, the time of eye opening (Sandmann et al., 1997).

Two continuous distinct bands of ChAT-IR processes were clearly seen in the outermost and innermost strata of the IPL at P3. Horizontal cells exhibited transient ChAT-IR in the rat retina from P4 to P10 (present study; Kim et al., 1998a), before the development of synapses at P6 in the OPL and at P12 in the IPL (Weidman and Kuwabara, 1968; Horsburgh and Sefton, 1987). In addition, the number of ChAT-IR cells increased steadily until P15, with their numbers decreasing thereafter. It is significant that there were major increases in ChAT-IR cells during 1) the perinatal period, 2) between P5 and P7, and 3) between P10 and P15. These three periods coincide closely with those found by Potts et al. (1982), who have shown that the number of ganglion cells reaches a near-adult value in the perinatal period, with the first appearance of synapses in the OPL at P5 and P7, and with the first appearance of synapses in the IPL between P10 and P15 (Weidman and Kuwabara, 1968; Horsburgh and Sefton, 1987). Taken together, our results suggest that ACh produced by cholinergic cells may play important roles in retinal maturation. This view is supported by evidence that ACh is necessary for synapse formation (Lipton and Kater, 1989) and that ACh is an important neuroactive substance in ontogeny, involved in early migration and process outgrowth (Lipton and Kater, 1989; Wong, 1995; Redburn and Rowe-Rendleman, 1996).

In the present study, the overall numbers of ChAT-IR cells decreased gradually from P15 onward. These results could be due to loss of the ChAT phenotype or to actual death of cholinergic cells. It is generally considered that large numbers of amacrine cells in the INL and GCL of the rat retina are casualties of a wave of cell deaths during the second postnatal week (Beazley et al., 1987; Horsburgh and Sefton, 1987). Thus, although the loss of the ChAT phenotype may be a major reason for the decline in ChAT-IR cells, it cannot be excluded that the decrease could also be attributed to actual cell death, considering the report by Braekevelt and Hollenberg (1970), who have shown that the thickness of the INL and GCL decreases from P15 to adulthood.

Comparison with development of GABA-IR amacrine cells

γ-Aminobutyric acid (GABA) is a major inhibitory neurotransmitter of amacrine cells (Brecha, 1983; Massey and Redburn, 1987; Wässle and Boycott, 1991; Freed, 1992). GABA has been identified as a significant component in the mechanism of directional selectivity, which is mediated by the $GABA_A$ receptor (Barlow and Levick, 1965; Wyatt and Daw, 1975; Ariel and Daw, 1982; Amthor and Grzywacz, 1993; Kittila and Massey, 1997; Massey et al., 1997). Based on the neuroactive substances they contain, GABAergic amacrine cells can be classified into several subtypes. The cholinergic amacrine cells have been identified as a subtype of GABAergic amacrine cells (Brecha et al., 1988; Chun et al., 1988; Kosaka et al., 1988; Vaney and Young, 1988; Masland et al., 1989; O'Malley and Masland, 1989; Vaney, 1990; Massey et al., 1991; Wässle and Boycott, 1991; Freed, 1992).

However, in the rat retina, the developmental pattern of the GABAergic amacrine cell is quite different from that of the cholinergic amacrine cell, and this difference is significant. First, the timing of the advent of the two cells is different: ChAT-IR amacrine cells appear first at E17, whereas GABA-IR or ^{3}H-GABA-labeled amacrine cells are first detected at birth (Versaux-Botteri et al., 1989; Oh et al., 1995; Fletcher and Kalloniatis, 1997). This discrepancy might be due to the slightly different roles of acetylcholine and GABA during retinal development. Support for this view comes from evidence that GABA may be involved in synaptogenesis at intermediate stages of retinal development (Redburn, 1992; Redburn and Rowe-Rendleman, 1996; Fletcher and Kalloniatis, 1997), after acetylcholine has played its roles in early interactions with migrating cytoblasts and triggering the outgrowth of processes (Redburn and Rowe-Rendleman, 1996). Second, the time course of development is different. At E17, ChAT immunoreactivity was observed in a sparse population of displaced cholinergic neurons in the GCL; the population of conventional ChAT-IR cells did not appear until P0. In contrast, it has been reported that GABA-immunoreactivity was observed in a sparse population of conventional amacrine cells at birth,

and in a displaced population by P4 (Oh et al., 1995; Fletcher and Kalloniatis, 1997). These timing differences between ChAT-IR and GABA-IR amacrine cells suggest that cholinergic amacrine cells have a unique developmental course that is independent of that of GABAergic amacrine cells during early retinal development.

The acquisition of the GABA phenotype by the cholinergic amacrine cell implies the completion of functional maturation, taking into consideration the role of GABA in the directional selectivity of adult rabbit retina (for reviews, see Masland and Tauchi, 1986; Vaney, 1990; Wässle and Boycott, 1991). It is reported that, at P6, GABA-IR amacrine cells appeared to form two distinct strata within the IPL, which might be putative strata of cholinergic amacrine cells, and that, around the age of eye opening, the retina was neurochemically similar to that of the adult (Oh et al., 1995; Fletcher and Kalloniatis, 1997). Furthermore, the development of the electroretinogram is thought to be functionally completed at eye opening (Weidman and Kuwabara, 1968). Thus, these cholinergic amacrine cells might acquire an ability to express the GABA phenotype from around P6 to the time of eye opening. Based on our preliminary data with double-labeling immunocytochemistry, 94.7% of ChAT-IR cells (36/38) exhibited GABA-immunoreactivity at P10 (unpublished data). However, further studies are clearly required to determine the precise time when cholinergic amacrine cells express the GABA phenotype.

ACKNOWLEDGMENTS

We are grateful to H.-D. Rho and B.-W. Hong for their technical assistance.

LITERATURE CITED

Amthor FR, Grzywacz NM. 1993. Inhibition in On-Off directionally selective ganglion cells in the rabbit retina. J Neurophysiol 69:2174-2187.

Ariel M, Daw NM. 1982. Pharmacological analysis of directionally sensitive rabbit retinal ganglion cells. J Physiol (Lond) 324:161-185.

Barlow HB, Levick WR. 1965. The mechanism of directionally selective units in rabbit's retina. J Physiol (Lond) 178:477-504.

Beazley LD, Perry VH, Baker B, Darby JE. 1987. An investigation into the role of ganglion cells in the regulation of division and death of other retinal cells. Brain Res Dev Brain Res 33:169-184.

Boycott B, Wässle H. 1999. Parallel processing in the mammalian retina. Invest Ophthalmol Vis Sci 40:1313-1327.

Braekevelt CR, Hollenberg MJ. 1970. The development of the retina of the albino rat. Am J Anat 127:281-302.

Brandon C. 1987. Cholinergic neurons in the rabbit retina: dendritic branching and ultrastructural connectivity. Brain Res 426:119-130.

Brecha N. 1983. Retinal neurotransmitters: histochemical and biochemical studies. In:Emson PC, editor. Chemical neuroanatomy. New York: Raven Press. p 85-129.

Brecha NC, Johnson D, Peichl L, Wässle H. 1988. Cholinergic amacrine cells of the rabbit retina contain glutamate decarboxylase and gamma-aminobutyrate immunoreactivity. Proc Natl Acad Sci USA 85:6187-6191.

Camargo L, Campos DM, Hokoç JN. 1999. Ontogeny of cholinergic amacrine cells in the opossum (*Didelphis aurita*) retina. Int J Dev Neurosci 17:795-804.

Cepko CL. 1993. Retinal cell fate determination. Prog Ret Res 12:1-12.

Cepko CL, Austin CP, Yang X, Alexiades M, Ezzeddine D. 1996. Cell fate determination in the vertebrate retina. Proc Natl Acad Sci USA 93: 589-595.

Chun M-H, Wässle H, Brecha N. 1988. Colocalization of [^{3}H] muscimol uptake and choline acetyltransferase immunoreactivity in amacrine cells of the cat retina. Neurosci Lett 94:259-263.

Conley MD, Fitzpatrick D, Lachica EA. 1986. Laminar asymmetry in the distribution of choline acetyltransferase-immunoreactive neurons in the retina of the tree shrew (*Tupaia belangeri*). Brain Res 399:332-338.

Dann JF. 1989. Cholinergic amacrine cells in the developing cat retina. J Comp Neurol 289:143-155.

Famiglietti EV. 1983. "Starburst" amacrine cells and cholinergic neurons: mirror-symmetric ON and OFF amacrine cells of rabbit retina. Brain Res 261:138-144.

Famiglietti EV, Tumosa N. 1987. Immunocytochemical staining of cholinergic amacrine cells in rabbit retina. Brain Res 413:389-403.

Feller MB, Wellis DP, Stellwagen D, Werblin FS, Shatz CJ. 1996. Requirement for cholinergic synaptic transmission in the propagation of spontaneous retinal waves. Science 272:1182-1187.

Fletcher EL, Kalloniatis M. 1997. Localization of amino acid neurotransmitters during postnatal development of the rat retina. J Comp Neurol 380:449-471.

Freed MA. 1992. GABAergic circuits in the mammalian retina. Prog Brain Res 90:107-131.

Horsburgh GM, Sefton J. 1987. Cellular differentiation and synaptogenesis in the developing retina of the rat. J Comp Neurol 263:553-566.

Kim I-B, Park D-K, Oh S-J, Chun M-H. 1998a. Horizontal cells of the rat retina show choline acetyltransferase- and vesicular acetylcholine transporter-like immunoreactivities during early postnatal developmental stages. Neurosci Lett 253:83-86.

Kim I-B, Oh S-J, Na W-K, Lee M-Y, Chun M-H. 1998b. Distribution pattern and synaptic circuitry of cholinergic neurons in the rat retina. Korean J Anat 31:136-150.

Kittila CA, Massey SC. 1997. Pharmacology of directionally selective ganglion cells in the rabbit retina J Neurophysiol 77:675-689.

Kosaka T, Tauchi M, Dahl JL. 1988. Cholinergic neurons containing GABA-like and/or glutamic acid decarboxylase-like immunoreactivities in various brain regions of the rat. Exp Brain Res 70:605-617.

Koulen P. 1997. Vesicular acetylcholine transporter (VAChT): a cellular marker in rat retinal development. Neuroreport 8:2845-2848.

Lipton SA, Kater SB. 1989. Neurotransmitter regulation of neuronal outgrowth, plasticity and survival. Trends Neurosci 12:265-270.

Mariani AP, Hersh LB. 1988. Synaptic organization of cholinergic amacrine cells in the rhesus monkey retina. J Comp Neurol 267:269-280.

Masland RH. 1977. Maturation of function in the developing rabbit retina. J Comp Neurol 175:275-286.

Masland RH, Tauchi M. 1986. The cholinergic amacrine cell. Trends Neurosci 9:218-223.

Masland RH, Cassidy C, O'Malley DM. 1989. The release of acetylcholine and GABA by neurons of the rabbit retina. In: Weiler R, Osborne NN, editors. Neurobiology of the inner retina, NATO ASI Series, vol H 31. Berlin: Springer. p 15-26.

Massey SC, Redburn DC. 1987. Transmitter circuits in the vertebrate retina. Prog Neurobiol 28:55-96.

Massey SC, Blankenship K, Mills SL. 1991. Cholinergic amacrine cells in the rabbit retina accumulate muscimol. Vis Neurosci 6:113-117.

Massey SC, Linn DM, Kittila CA, Mirza W. 1997. Contributions of $GABA_A$ receptors and $GABA_C$ receptors to acetylcholine release and directional selectivity in the rabbit retina. Vis Neurosci 14:939-948.

Mitrofanis J, Stone J. 1988. Distribution of cholinergic amacrine cells in the retinas of normally pigmented and hypopigmented strains of rat and cat. Vis Neurosci 1:367-376.

Mitrofanis J, Maslim J, Stone J. 1988. Catecholaminergic and cholinergic neurons in the developing retina of the rat. J Comp Neurol 276:343-359.

Mitrofanis J, Maslim J, Stone J. 1989. Ontogeny of catecholaminergic and cholinergic cell distribution in the cat's retina. J Comp Neurol 289:228-246.

Oh S-J, Lee M-Y, Chun M-H. 1995. Localization and coexistence of GABA and dopamine in the retinal neurons of the developing and adult rats. Korean J Anat 28:607-621.

O'Malley DM, Masland RH. 1989. Corelease of acetylcholine and gamma-aminobutyric acid by a retinal neuron. Proc Natl Acad Sci USA 86: 3414-3418.

Potts RA, Dreher B, Bennett MH. 1982. The loss of ganglion cells in the developing retina of the rat. Brain Res Dev Brain Res 3:481-486.

Pourcho RG, Osman K. 1986. Cytochemical identification of cholinergic amacrine cells in the cat retina. J Comp Neurol 247:497-504.

Puro DG, Batelle BA, Hansmann KE. 1982. Development of cholinergic neurons of the rat retina. Dev Biol 91:138-148.

Redburn DA. 1992. Development of GABAergic neurons in the mammalian retina. Prog Brain Res 90:133-147.

Redburn DA, Rowe-Rendleman C. 1996. Developmental neurotransmitters. Invest Ophthalmol Vis Sci 37:1479-1482.

Rodieck RW, Marshak DM. 1992. Spatial density and distribution of choline acetyltransferase immunoreactive cells in human, macaque, and baboon retinas. J Comp Neurol 321:46-64.

Sandmann D, Engelmann R, Peichl L. 1997. Starburst cholinergic amacrine cells in the tree shrew retina. J Comp Neurol 389:161-176.

Schmidt M, Wässle H, Humphrey M. 1985. Number and distribution of putative cholinergic neurons in the cat retina. Neurosci Lett 59:235-240.

Sernagor E, Grzywacz NM. 1996. Influence of spontaneous activity and visual experience on developing retinal receptive fields. Curr Biol 6:1503-1508.

Vaney DI. 1990. The mosaic of amacrine cells in the mammalian retina. Prog Ret Res 9:49-100.

Vaney DI, Young HM. 1988. GABA-like immunoreactivity in cholinergic amacrine cells of the rabbit retina. Brain Res 438:369-373.

Vaney DI, Peichl L, Boycott BB. 1981. Matching populations of amacrine cells in the inner nuclear and ganglion cell layers of the rabbit retina. J Comp Neurol 199:373-391.

Versaux-Botteri C, Poche R, Nguyen-Legros J. 1989. Immunohistochemical localization of GABA-containing neurons during postnatal development of the rat. Invest Ophthalmol Vis Sci 30:652-659.

Voigt T. 1986. Cholinergic amacrine cells in the rat retina. J Comp Neurol 248:19-35.

Wässle H, Boycott BB. 1991. Functional architecture of the mammalian retina. Physiol Rev 71:447-480.

Weidman TA, Kuwabara T. 1968. Postnatal development of the rat retina. An electronmicroscopic study. Arch Ophthalmol 79:470-484.

Wong ROL. 1995. Cholinergic regulation of $[Ca^{2+}]_i$ during cell division and differentiation in the mammalian retina. J Neurosci 15:2696-2706.

Wong ROL, Collin SP. 1989. Dendritic maturation of displaced putative cholinergic amacrine cells in the rabbit retina. J Comp Neurol 287:164-178.

Wyatt HJ, Daw NW. 1976. Specific effects of neurotransmitter antagonists on ganglion cells in rabbit retina. Science 191:204-205.